On-Road Vehicle Trajectory Collection and Scene-Based Lane Change Analysis: Part II

Wen Yao, Qiqi Zeng, Yuping Lin, Donghao Xu, Huijing Zhao, *Member, IEEE*, Franck Guillemard, Stéphane Geronimi, and François Aioun

***Abstract*—This two-part paper aims to study lane change behaviors at the tactical level from an on-road perspective. Compared with longitudinal driving tasks, a lane change is more complicated because this task has more interactions with surrounding vehicles; thus, there are more potential risks during this procedure. Based on the results from Part I on an on-road vehicle trajectory collection, this part investigates lane change extraction and scene-based behavior analysis, and it has a particular focus on understanding the interactions between an ego and surrounding vehicles during the procedure. We claim that this paper provides the following novel contributions: 1) an automatic method is proposed for extracting lane change segments from a continuous driving sequence by modeling and recognizing patterns in a steering angle; 2) a lane change database at the trajectory level is generated, which reflects the interactions between an ego and the surrounding vehicles during the procedures; and 3) we present findings from analyzing lane change procedures using real-world data on the axes of both the ego's trajectory and interactions with the scene vehicles. To the authors' knowledge, this is the first lane change behavior study from an on-road perspective that addresses the vehicle interactions in real-world traffic at the trajectory level.**

***Index Terms*—Driving behavior, lane change, scene-based analysis, vehicle interaction, trajectory.**

I. Introduction

DRIVING is a daily activity, yet it is also a highly complex task. For decades, considerable research efforts have been devoted to studying the mechanism, which is generally identified in a hierarchical framework with three levels of processes, i.e., operational processes that involve manipulating control inputs for stable driving, tactical processes that govern safe interactions with the environment and other vehicles, and strategic processes for higher level reasoning and planning [1]. With the development of ADAS (Advanced Driver Assistance System) and autonomous driving systems, there are increasing needs for understanding complex driving behaviors at the tactical level, e.g., how a driver/vehicle performs a lane change maneuver with safe interactions with other traffic participants.

This two-part work aims to study lane change behaviors at the tactical level from an on-road perspective, and it has a particular focus on analyzing the interactions between an ego and the surrounding vehicles during the procedure. Compared with longitudinal driving tasks, such as car following or lane keeping, a lane change is more complicated because it makes a lateral shift on its path, has more interactions with surrounding vehicles, and thus possesses more potential risks during the procedure. We employ the approach depicted in Fig. 1, which consists of studies at four levels. Part I addresses the signal and trajectory levels, in which a system of all-around vehicle trajectory collection through on-road driving in real-world traffic is proposed, and the resulting trajectories through long-term on-road driving under changing traffic conditions and across large areas are demonstrated to have the necessary properties for tactical driving behavior studies. Based on the results, this work focuses on the semantic and behavioral levels. For this purpose, an automated method for lane change extraction from a continuous driving sequence is proposed, and an on-road database is subsequently developed, in which each data entry contains the trajectories of both the ego and environmental vehicles during the entire procedure of a lane change. They are analyzed on the axes of both the ego's lane change trajectories and the interactions with scene vehicles.

We claim that this paper provides the following novel contributions: 1) An automatic method is developed for extracting lane change segments, i.e., detecting the starting and ending time points of a lane change from a continuous driving sequence by modeling and recognizing patterns in steering angle without relying on a driver's indication. 2) A lane change database at the trajectory level is generated through large-scale on-road data collection and processing, and this database contains more than 1000 lane change data samples that describe interactions at the trajectory level between an ego and surrounding vehicles during the entire lane change procedure. 3) Lane change procedures are analyzed, from which a trajectory model is developed by cross-correlating the spatial-temporal features on the trajectory's end location and speed, and an interaction model is developed to classify lane changes and predict their interactions by cross-correlating the ego with other scene vehicles. To the authors' knowledge, this is the first study on lane change behaviors from an on-road perspective that addresses vehicle interactions in real-world traffic at the trajectory level. The findings will help in developing future

Manuscript received August 21, 2015; revised March 1, 2016 and April 30, 2016; accepted May 7, 2016. Date of publication July 7, 2016; date of current version December 23, 2016. This work was supported in part by the PSA's OpenLab program, by the National Natural Science Foundation of China under Grant 61573027, and by the Hi-Tech Research and Development Program of China under Grant 2012AA011801. The Associate Editor for this paper was F.-Y. Wang.

W. Yao, Q. Zeng, Y. Lin, D. Xu, and H. Zhao are with the Key Laboratory of Machine Perception (Ministry of Education), Peking University, Beijing 100871, China (e-mail: zhaohj@cis.pku.edu.cn).

F. Guillemard, S. Geronimi, and F. Aioun are with Groupe PSA (Peugeot Société Anonyme), 78943 Velizy, France.

Color versions of one or more of the figures in this paper are available online at http://ieeexplore.ieee.org.

Digital Object Identifier 10.1109/TITS.2016.2571724

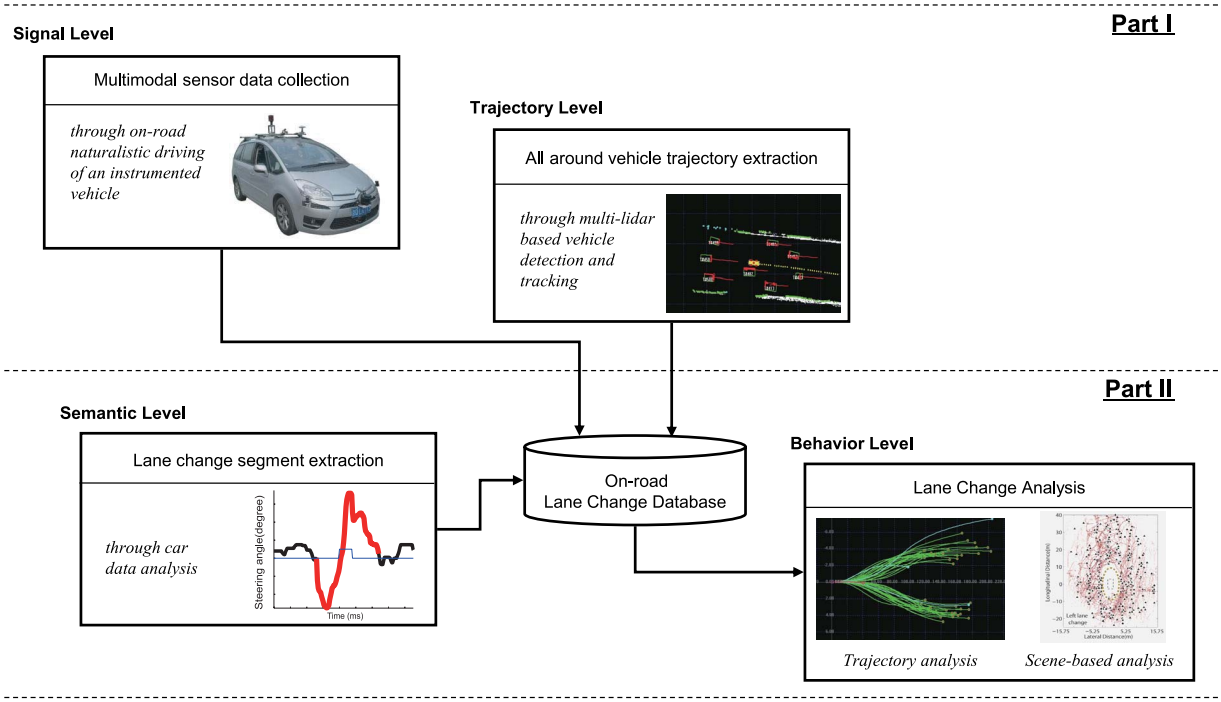

Fig. 1. Research structure.

ADAS or autonomous driving systems to govern safe and gentle social behaviors in dynamic traffic.

The remainder of this paper is organized as follows. A literature review is presented in Section II. The automatic method for extracting lane change segments from a continuous driving sequence using the vehicle's steering angle data is introduced in Section III. The lane change database is described in Section IV, which is developed based on a large amount of on-road driving experiments in real-world traffic. We present the findings from analyzing lane change procedures in the real-world data in Section V on the axes of both the ego's trajectory and interactions with the scene, followed by conclusions and future works in Section VI.

II. Related Work

Following the success in analyzing a vehicle's longitudinal behavior, such as lane keeping [2], [3] and platooning [4], [5], researchers are currently paying increasingly more attention to driving behaviors that involve lateral control, such as lane changes. Compared to the longitudinal ones, lane change behavior is more complex because its path contains both lateral and longitudinal movements, speed control may occur simultaneously with the headway management, and, more importantly, the decision making and maneuvers are highly correlated with the environments, such as the other traffic participants nearby. Broadly speaking, the studies are conducted on two major axes: lane change trajectory and behavioral reasoning in real-world traffic.

Reference [6] focused on modeling the path of lane changes, and [7]–[10] combined both velocity and path planning to generate lane change trajectories using parametric curve models that consider a vehicle's dynamic constraints. Algorithms have been applied for motion planning of real autonomous vehicles [11], [12], in which a set of trajectories are first generated at a discretized configuration space, and a trajectory is then selected that optimizes an objective function considering factors such as collision avoidance, time, distance, and acceleration. Extensions of these works can also be found in [13]–[16]. In these systems, scene dynamics are not concerned in trajectory generation, with the surrounding moving objects being modeled only to filter out the unsafe ones at the trajectory selection procedure. This is not exactly the same as the behaviors in real-world traffic, in which a driver governs its operation not only to avoid collisions but also with close interactions with its surroundings, and the resulting trajectories of lane change maneuvers are different depending on the location, speed and acceleration of the nearby vehicles, as well as the ego's state and the driver's personal properties. Furthermore, defining and discretizing the configuration space are not trivial tasks. If the configuration space is coarse-grained, the algorithm may fail in finding a proper trajectory for operation, whereas a find-grained configuration space results in a high computation cost that is not favorable for on-line processing. Moreover, such a strategy is not efficient because a driver's behavior may follow habitual patterns that are not fully considered in the methods.

Data is crucial in modeling and reasoning the lane change behaviors in real world traffic, where the use of a driving simulator or an instrumented vehicle or trajectory data through infrastructure sensing are among the major approaches. By using a driving simulator, the data regarding driving in a critical, dangerous or even crashed situation can be safely collected in a simulated environment, and it is easy to repeat an experiment under the same conditions with all parameters known [17], [18]. State-of-the-art driving simulators are able to realistically reproduce a real-world environment in a virtual space; however,

they lack accuracy in simulating the behaviors of moving objects, particularly their interactions. For studying the lane change behaviors, where considerable interactions happen in between an ego and surrounding vehicles, the models developed by using the data from a current driving simulator may lack of accuracy [19] in real-world situations. On the other hand, trajectory data sets have been developed through video processing by using the data from an airborne or infrastructure-based camera [20] to support for tactical driving behavior studies, where each data set contains the vehicle trajectories across a road section. In this area, the NGSIM (The Next Generation Simulation Program) [21] is among the most notable programs, and the resultant trajectory sets have been widely exploited: it provides a good basis for validation and calibration of the microscopic traffic models [23], [24]; [22] investigates and compares the traffic flow characteristics, which influence the lane changing behavior of heavy vehicle and passenger car drivers on freeways under heavy traffic conditions; [25] develops a model of predicting drivers lane-changing decisions that addressing the characteristic of traffic flow; [26] evaluates the impact of heavy vehicles to surrounding traffic.

Instrumented vehicles have been used for driving behavior study too, which are mounted by multi-modal sensors to monitor the driver, road and traffic. Many of these researches aim at online reasoning by using the current or a short period of history data for such as driving state awareness, motion prediction and risk assessment for autonomous driving or ADAS systems [27]. An early work can be traced to the SmartCar project [28], where emphasizing that driving context is an important factor that affects a driver and subsequently an ego-vehicle's behavior, on-road data consisting of the environmental vehicles, lane markings, driver's head and gaze, and the ego vehicle's parameters are collected using an instrumented vehicle equipped with four on-board video cameras. The data are used in the development of a graphical model for recognizing a driver's behaviors, such as pass, lane change, turn, stop, and start. Recent works can be found at [29], [30], where lane changes are predicted by training classifiers using the features on such as the driver's head motion, lane and the ego vehicle's parameters; [31], where the performance of lane change prediction is improved by using feature ranking with maximized predictive power; [32], where lane change risk is assessed by integrated modeling of the driver's gaze and operational behaviors. Research effort has also been found on modeling the different lane change styles on the parameters of duration and gap acceptance [33]. In recently years, NDS (Naturalistic Driving Study) have involve great efforts, among which the 100-Car NDS [34], SHRP2 [35], ANDS [36] and UDRIVE [37] are the most notable programs, where hundreds of instrumented vehicles with multi-modal sensors are developed and driven during participants' daily travel across years to collect real world data. The data have been analyzed to detect lane change events and assess drive quality [38]–[40]. In these NDS programs, cameras are used as the major exteroceptive sensors looking in and outside the ego, while no trajectory data is collected and analyzed of the scene vehicles.

In order to model the lane change trajectories in real world traffic and analyze the interactions between an ego and surrounding vehicles for behavioral reasoning, a trajectory-based study from an on-road perspective is important. Based on the results of Part I, where high-quality trajectories that contain both an ego and all interacting vehicles are collected through on-road driving, this work contributes to the methods of automated lane change trajectory extraction, real-world database generation and scene-based lane change analysis. An early report of this work can be found at [41], while the methods has been greatly refined with extensive experimental data analysis.

III. Lane Change Extraction

On-road driving is a continuous procedure, and it can be symbolically described as a sequence of different behaviors. However, a challenge is that there is no clear "delimiter" in the consecutive data frames. To study each type of behavior, an automatic algorithm to detect and extract the data segments is crucial. This work begins with the studies of lane change behaviors on straight roads, which can be extended to curved road maneuvers by addressing road geometry. Herewith we provide the following definitions.

Definition 1: A *lane change segment* is defined by a pair of start and end time points, which meet the following conditions.

1) The ego heads to the road direction at the start and end time points.
2) The ego has a lateral shift of approximately a lane width during the period.
3) It is the shortest period that meets the above two constraints.

Definition 1': A *lane change segment* on a straight road is defined following the Definition 1 with an amendment to the first condition.

1) The ego heads to the same direction at the start and end time points.

Definition 2: Given a time series of data frames $\{f_i\}_{i=t_0\sim t_n}$, *lane change extraction* is to detect all lane changes $C_{1,\ldots,m}$ and estimate the corresponding start and end time points $C_k = [t_s, t_e]_k$ that meet the conditions of Definition 1.

Lane changes can primarily be inferred from three types of cues, namely, a driver's indication, correlations with lane and steering wheel handling. Considering that a driver may not provide an indication for some of the lane changes and that correlation with the lane may have problems when lane markers are unclear or occluded, this study propose an automatic method for lane change segment extraction by modeling and recognizing patterns in the vehicle's steering angle data. However, in developing a system for real-world applications, it is suggested that all of the above cues be used to improve the efficiency and accuracy.

Below, we model lane change pattern in Section III-A, and present the automated extraction method in Section III-B. The issue of feature definition is not trivial, which is analyzed in Section III-C, followed by the experimental results and discussions in Section III-D.

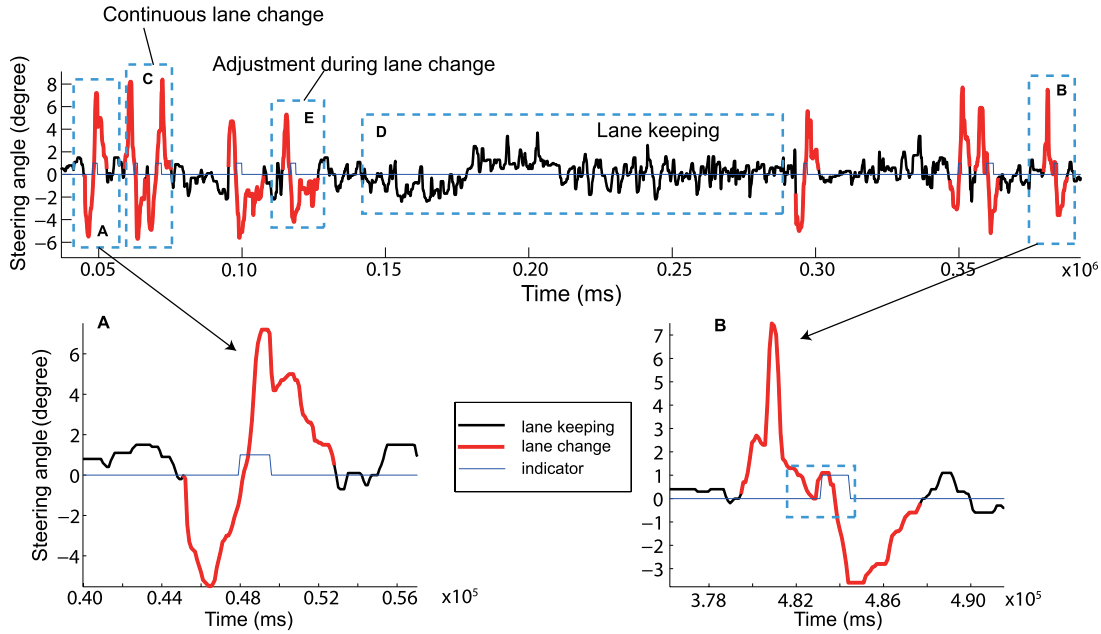

Fig. 2. Steering angle sequences of lane change segments. A–B: a right and left lane change.

A. Lane Change Pattern Modeling

Turning steering wheel is a driver's major operation during a lane change, and this operation is captured in the car's steering angle data. Fig. 2 shows a data sequence with a number of typical cases marked. Turning left outputs positive values, while turning right are negatives. Cases A and B are the sequences of left and right lane changes, while case C is composed of two consecutive lane changes in opposite directions, representing an overtaking behavior.

In the steering angle data, a standard lane change segment is composed of two consecutive parts of steering operation in opposite directions. For example, in conducting a right lane change, a driver will first steer to the right to cross the lane, and then steer to the left to head toward the road direction. Both operations are normally finished rapidly within several seconds with a steering velocity much higher than the other operations in headway managements. However, a driver's operation may not always be standard, and most real-world data are not as ideal as that of case A. In case B, a small data peak exists between the two major steering operations. It has been discovered that a driver may tune the steering wheel due to overshooting or interference from the vehicles in the target lane, or keep it in a neutral position for a while (called "gap time" below) that corresponds to a behavior of cross-lane driving.

A lane change segment of the steering angle data is modeled in Fig. 4, with the most significant parameters listed in Table I, and the properties defined below. However these parameters are correlated. They are selectively incorporated in training a classifier for lane change extraction.

Definition 3: A straight road lane change segment in the steering angle data is *modeled* below.

1) Two turning operations are of symmetry in (t_1, t_2), $(|\alpha_1|, |\alpha_2|)$, $(|p_1|, |p_2|)$ and $(|\omega_1|, |\omega_2|)$.
2) Shorter a t_0 w.r.p. to the entire operation time, more confidence in pairwising the two turning operations.
3) Road geometry is reflected by $\alpha_1 + \alpha_2$. On a straight road, $\alpha_1 + \alpha_2 \approx 0$.
4) Personal deviations exist in the absolute values as well as the difference of (t_1, t_2), $(|p_1|, |p_2|)$ and $(|\omega_1|, |\omega_2|)$.

B. Lane Change Extraction

As outlined in Fig. 3, lane change extraction consists of three modules: candidate generation, online lane change validation and offline classifier training. Given a time series of steering angle data, lane change candidates are generated through the following steps: 1) Operation labeling is of thresholding on the steering angle data, and labeling each data frame into L_{left}, L_{right} and L_{neutral} for its handling operations. As depicted by the case D of Fig. 2, although the car performed lane keeping, fluctuations exist in the steering angle data. With this processing, the handlings above a significant level are extracted. 2) Segmentation is conducted on the sequence of operation labels. For each segment, the parameters of α and t as defined in Table I are estimated, the segments having parameters within predefined threshold values are extracted and associated with labels of M_{left} and M_{right} to indicate the turning operations. 3) In candidate generation, the pairs of successive segments are detected that are associated with the labels of opposite turning operations and with a gap time t_0 shorter than a threshold. Candidates are generated of C_{right} for a right lane change on the pair of $(M_{\text{right}}, M_{\text{left}})$ and C_{left} for a left one on $(M_{\text{left}}, M_{\text{right}})$. In case of confusing situations, candidates are generated on all combinations.

Candidate generation is shared by both online and offline procedures. In the offline procedure, the candidates are examined by an operator on an on-board video. The correct ones are labeled as the positive samples, and the wrong ones are negatives. These samples are used in training an SVM-based classifier that is used in online processing to examine each candidate for lane change detection.

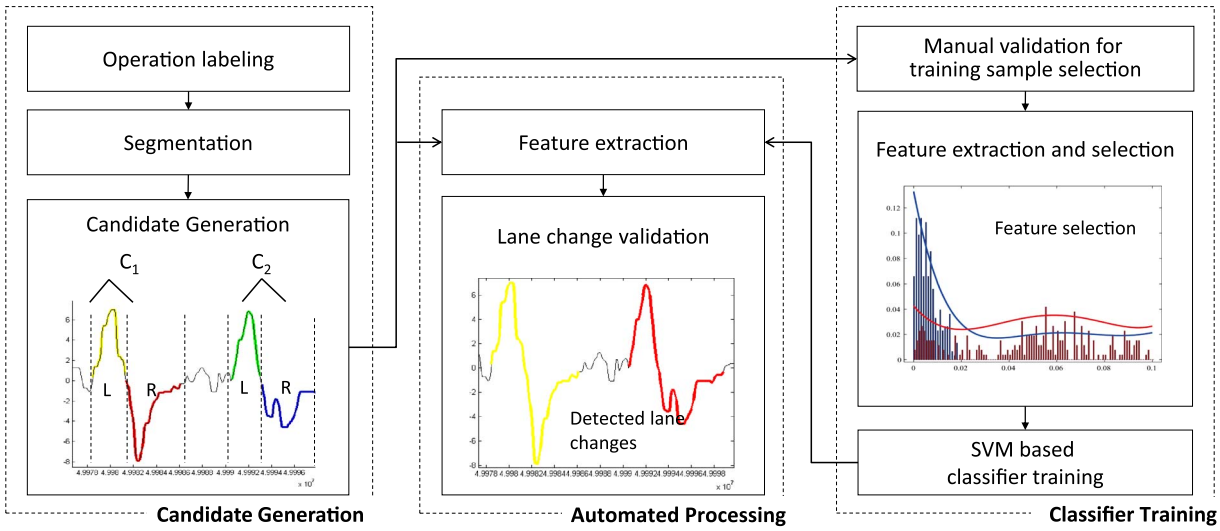

Fig. 3. Processing flow of lane change extraction.

TABLE I
PARAMETER DEFINITION FOR LANE CHANGE MODELING

Definition	Description
t_0	gap time in between of the two opposite turning op.
$t_{1,2}$	duration time of the 1st and 2nd turning op.
$p_{1,2}$	the pick steering angle values (i.e. the significance) of the 1st and 2nd turning op.
$\alpha_{1,2}$	$= \int_0^{t_{1,2}} p_t dt$, integration of the steering angles ($\propto$ heading angle changes) in the 1st and 2nd turning op.
$\omega_{1,2}$	$= p_{1,2}/\Delta T_{1,2}$, initial steering velocities of the 1st and 2nd turning op.

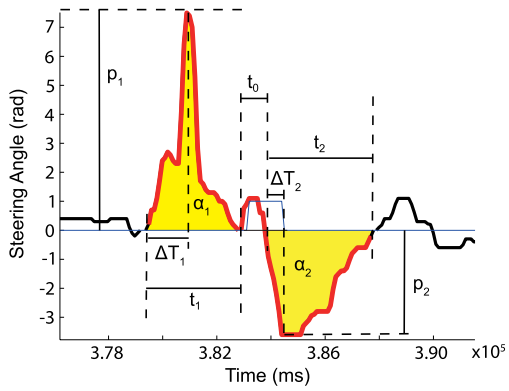

Fig. 4. Lane change modeling on steering angle data.

TABLE II
FEATURE DEFINITION FOR LANE CHANGE EXTRACTION

Feature	Definition	Description
1	$t_0/(t_1+t_2)$	ratio of the gap time to the total time of two turning op.
2	t_1/t_2	ratio of the 1st turning op. time to the 2nd one
3	$t_0+t_1+t_2$	duration time of the lane change
4	$\lvert\alpha_1/\alpha_2\rvert$	absolute ratio of the 1st heading angle change to the 2nd one
5	$\lvert\alpha_1+\alpha_2\rvert$	absolute heading angle change after the two turning op.
6	$\max(\lvert\alpha_1\rvert,\lvert\alpha_2\rvert)$	the largest heading angle change of the two turning op.
7	$\lvert p_1/p_2\rvert$	absolute ratio of the largest steering angle of the 1st turning op. to the 2nd
8	$\max(\lvert p_1\rvert,\lvert p_2\rvert)$	absolute value of the largest steering angle of the maneuver
9	d_{lat}	lateral shift during the procedure
10	$\lvert\omega_1/\omega_2\rvert$	ratio of the steering velocities of the 1st turning op. to the 2nd
11	$\max(\lvert\omega_1\rvert,\lvert\omega_2\rvert)$	the largest steering velocity of the two turning op.

C. Feature Analysis

Due to the limited number of samples and noisy signal data, selecting the most significant features is crucial in avoiding the over-fitting problem in training a classifier for lane change extraction. In this research, eleven dominant features are defined as listed in Table II, addressing on the aspects of operation time, heading angle change, significance of steering operation, lateral shift and steering velocities. With the set of training samples consisting of both positive and negative ones, statistical analysis is conducted on the feature values to examine the distinctiveness. As shown in Fig. 5, for each feature, two histograms are developed on the values of positive and negative samples, and polynomial curves are subsequently fitted as shown in blue and red, respectively, which can be found of obvious distinctiveness. Below we analyze the fitting curves (blue) of positive sample values. Operation symmetry is evaluated by features 2, 4, 7 and 10, which are demonstrated by the blue curves with their pick values slightly less or more than 1.0 for features 2 and 7, just around 1.0 for feature 4. Although the blue curve of feature 10 has a pick value around 1.0, a large variance can be found on the histogram. It tells that symmetry on steering velocities is not as distinctive as those on the other features. On the other hand, feature 11 evaluates the absolute steering velocity values, where large variance can be found too. It means that steering velocity could vary largely on different lane change operations or the value could be sensitive to signal error. Feature 4 addresses on the ratio of heading angle changes that are constrained by road geometry. On straight roads, the ratios are 1.0 as the heading angle changes on two opposite directions are equal. The fact is demonstrated by the statistics. Features 5 and 9 concern the constraints on heading angle change and lateral shift after

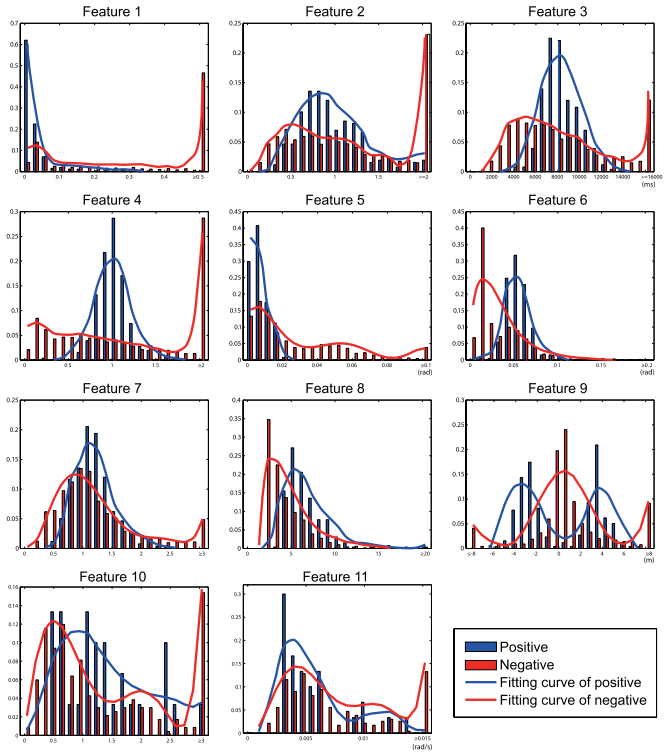

Fig. 5. Statistical analysis of the features.

the entire procedure, which have their pick values near 0 for feature 5 and 3.75 m for feature 9. Feature 1 serves as a confidence measure, i.e., smaller a value, more confidence in combining the two turning operations. Feature 3 addresses on the absolute values of duration time, which is demonstrated of a pick value at 8 s. However these features are correlated. For example, steering velocity (features 10 and 11) is correlated with the velocity of heading angle change, which is addressed collaboratively by the features 4–6 on heading angle change and 1–3 on duration time. In this research, a classifier is finally trained by combining features 1–9, while we compare the results with those using also other features.

D. Experimental Results

A test data is developed by using the on-road driving data at 3 different days that is described in the next section. Ground truth are generated by an operator by manually marking major segments of true lane changes on an on-board video. However, because it is difficult for an operator to locate their start and end times at sub-second accuracy, the manually labeled data are only used to count the numbers of true positives (TP), false positives (FP) and false negatives (FN) in the automated extraction results. Note that the ground truth data do not contain false lane changes; thus, there are no true negatives (TN) in this experiment. Below, we first analyze the result using some typical cases, then discuss the final results on the 3 days' data.

Five typical cases are selected as depicted in Fig. 6(a) with three columns for the labeling, segmentation and extraction results, respectively. As a reference, vehicle trajectories at a global frame during the period of the segment are presented in (b), where the ego is in yellow, and the environmental ones'

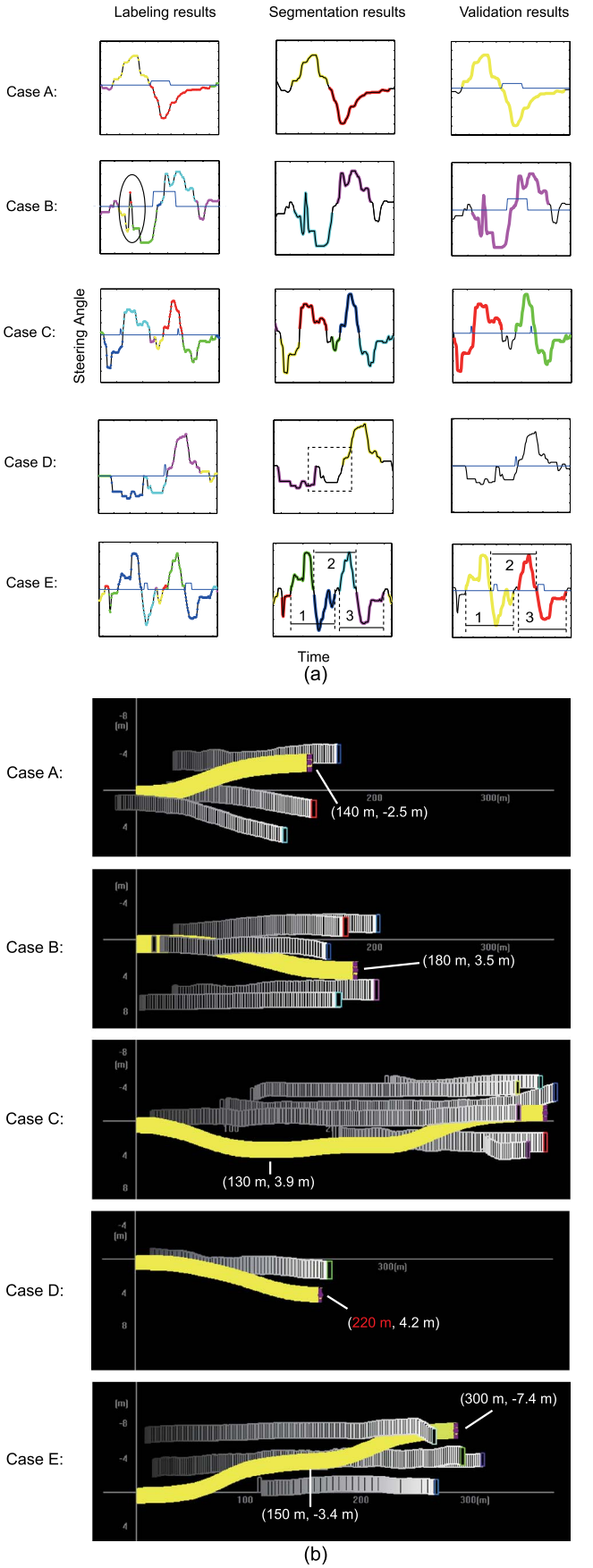

Fig. 6. Case study of lane change extraction results. (a) Results on steering angle data. (b) Visualization of the trajectories with the ego in yellow and others in gray.

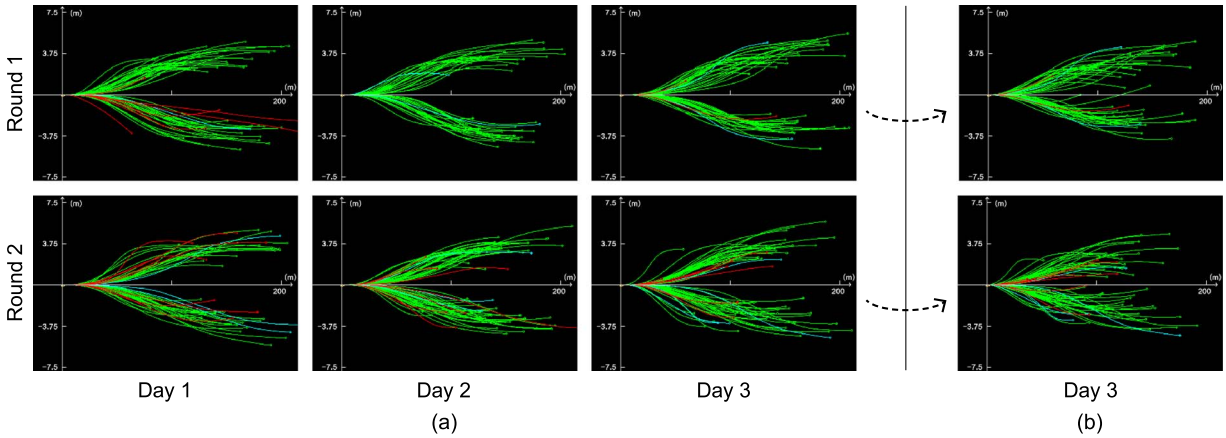

Fig. 7. Extracted lane change trajectories. (a) Results of automated extraction. (b) Results after the intentional shift of the start time of the lane change segments of D3-R1 and D3-R2 to 1 s later.

are in gray. Case A is a standard lane change, which has good symmetry in the two opposite turning maneuvers in both operation time and heading angle changes, and the signals have little fluctuation with no gap time in between the two consecutive turning maneuvers. In case B, there is a short data jump, where during the right turning operation, the driver quickly moved steering wheel back to a neutral position and then continued turning right. Such data jumps could occur in case of interference from the other cars of the scene. The segmentation method has addressed on such short fluctuation in a merge process, thus resulted in a succeeded lane change extraction. Case C is an overtaking behavior that has two consecutive lane changes in opposite directions as visualized in (b), where the yellow trajectory of the ego vehicle first changed to the right lane then merged back to the previous lane. As shown in (a), both lane changes are successfully extracted as drawn in different colors denoting their IDs. Cases D and E are the negative results. The data of case D within the dotted area in (a) failed in segmentation; thus, these data were treated as the gap time in between the two opposite turning operations, yielding a large value (0.7) for Feature 1, which is a major reason for its failure in validation. Case E is a behavior that contains two continuous lane changes in the same direction. The behavior can be more clearly observed in (b), where the yellow trajectory of the ego vehicle first changes to the second lane and then changes to the third lane. In this study, the algorithm is designed to generate candidates on all combinations. Thus, three candidates are generated on the data for case E, as illustrated by no. 1, 2 and 3, and all have passed validation. However, no. 2 is a negative.

Each lane change trajectory is aligned to a global frame (see Definition 6), and all extracted trajectories are plotted in Fig. 7(a), with the TPs in green, FPs in red and FNs in water blue. In order to demonstrate the importance of accurately extracting the time points, we intentionally shift the start time of each lane change segment to 1 second later and plot the results of two rounds in Day 3 in Fig. 7(b). It can be observed that the trajectories in the left column (i.e., the automated extraction results) are more regulated, and the general patterns are more clear, in accordance with definition 1.

In this research, two classifiers ($\mathcal{C}_9$ and $\mathcal{C}_{11}$) are trained on features 1–9 and 1–11 respectively, and their results are compared in Table III. D1, D2 and D3 denote the three different days, and each has R1 and R2 corresponding to the two driving experiments. For example, in D1-R2, the driver performed 41 lane changes, and they are marked as the ground truth data. With the classifier $\mathcal{C}_9$, 40 are extracted automatically (TP), 1 is missed (FN), and 8 others in the extraction results are counted as false detections (FP). Therefore, Precision $= \mathrm{TP}/(\mathrm{TP}+\mathrm{FP})$, Recall $= \mathrm{TP}/(\mathrm{TP}+\mathrm{FN})$ of this experiment are 83.33%, 97.56% respectively. Due to the small number of lane changes in each day-round, the experimental results contain considerable fluctuations. For the six experiments over three days, total results on each classifier are summarized with the highest values on precision and recall shown in bold. It can be found that $\mathcal{C}_{11}$ has high recall, while $\mathcal{C}_9$ is much precise. As has been found in feature analysis, symmetry on steering velocities (i.e., feature 10)

TABLE III
PRECISION AND RECALL OF THE EXTRACTION RESULTS

			TP	FP	FN	Precision(%)	Recall(%)
D1	R1	$\mathcal{C}_9$	49	4	0	92.45	100.00
		$\mathcal{C}_{11}$	48	6	1	88.89	97.96
	R2	$\mathcal{C}_9$	40	8	1	83.33	97.56
		$\mathcal{C}_{11}$	40	9	1	81.63	97.56
D2	R1	$\mathcal{C}_9$	39	5	4	88.64	90.70
		$\mathcal{C}_{11}$	42	3	1	93.33	97.67
	R2	$\mathcal{C}_9$	58	10	4	85.29	93.55
		$\mathcal{C}_{11}$	60	11	2	84.51	96.77
D3	R1	$\mathcal{C}_9$	47	6	2	88.68	95.92
		$\mathcal{C}_{11}$	48	7	1	87.27	97.96
	R2	$\mathcal{C}_9$	53	7	4	88.33	92.98
		$\mathcal{C}_{11}$	52	7	5	88.14	91.23
Total		$\mathcal{C}_9$	286	40	15	**87.73**	95.02
		$\mathcal{C}_{11}$	290	43	11	87.09	**96.35**

TABLE IV
ON-ROAD EXPERIMENTAL SETTING

Road Information	
Length per round	65.3 km
maximum design speed	80 km/h
Lane width	3.75 m
road properties	4 lanes each direction
Experiment setting	
2 rounds per day	10 days
Experiment time	1^{st} round: 10:00 am - 12:00 pm 2^{nd} round: 12:00 pm - 14:00 pm
Total length	1232 km
Total lane change behaviors recorded	1596
Valid lane change behaviors samples	1006

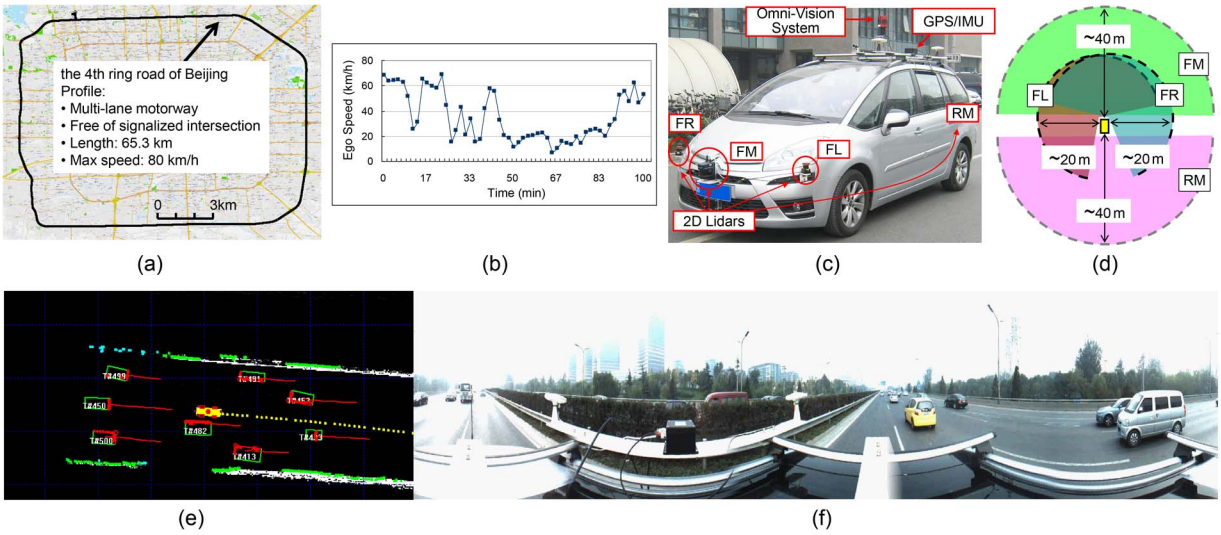

Fig. 8. On-road data collection. (a) Route of on-road driving. (b) Speed graph during one round driving. (c) Instrumented vehicle with multimodal sensors. (d) Ego-centered 360° sensing coverage. (e) On-road vehicle trajectory extraction. (f) Omni-image of the road condition.

is not as distinctive as those on the other features, and large variance exists in the steering velocity values (i.e., feature 11) of different lane change operations. These could be reasons for the reduced precision after incorporating the additional features 10 and 11. In this research, $\mathcal{C}_9$ is finally exploited in lane change extraction for high precision.

IV. Lane Change Database Generation

A large-scale on-road experiment is conducted, as described in Table IV. During the experiment, sensor data are collected while driving the instrumented vehicle as shown in Fig. 8 along the 4th ring road of Beijing, which is a multi-lane motorway with no signalized intersection, a total distance of 65.3 km and a designed maximum speed of 80 km/h. The road is composed of a square loop with mostly straight segments. It is a pleasant environment for this research, which begins with the study of lane changes on straight roads.

The experiments for on-road data collection are conducted by a single driver over the course of ten working days. Each day has two experiments, and in each experiment, on-board sensor data are collected across one round of driving on the 4th ring road of Beijing during non-rush hours, e.g., 10:00 am–12:00 pm and 12:00 pm–14:00 pm. Normally, it takes 100 min for driving one round. However, although the experiments were conducted during non-rush hours, the traffic conditions were not uniform but has considerable changes along the road. Because the instrumented vehicle is driven naturally, its speed reflects the nearby traffic conditions. A graph of the ego's speed during one round of driving is presented in Fig. 8(b). It can be observed that the speed dramatically changed, reflecting both jammed and free-flowing traffic conditions.

With the multi-modal sensor data collected through on-road driving, vehicle trajectories are extracted as described in Part I. Meanwhile, the car's data are processed to extract lane change segments by using the method described in the previous section. Because all these data are synchronized and geo-referenced into the same spatial-temporal coordinate system, with the start and end time points of each lane change segment, the vehicle trajectories during the period are extracted to compose data for a single lane change according to the following definition.

Definition 4: An *ego vehicle* is the subject of the study. The *ego vehicle* in the lane change data is the one that conducts a lane change. In this research, it is the instrumented vehicle.

Definition 5: An *ego frame* in the lane change data is defined with an origin at the center of the ego vehicle, a longitudinal axis in the direction of the vehicle's heading, a lateral one pointing to the vehicle's left, and a time axis pointing upward. t_s is set to be the origin of the time axis.

Definition 6: A *global frame* in the lane change data is defined by the Frenet Frame [8], with its origin at the ego's location at an initial time t_s of the lane change. A trajectory point at an offset time $t = t_r - t_s$ is denoted by $p_t = (s_t, d_t)$, representing its displacement from the origin on the road's longitudinal and lateral directions.

Definition 7: Lane change data contain a set of synchronized and geo-referenced trajectories, as defined below.

$$LC = \{T_{\text{Ego}}, T_{\text{CF}}, T_{\text{TF}}, T_{\text{TR}}, T_{\text{OE}_1}, \ldots, T_{\text{OE}_n}\}_{t_s}^{t_e}.$$

- Ego: the ego vehicle;
- CF: the front vehicle in the same lane with the ego vehicle;
- TF and TR: the front and rear vehicles in the target lane of the lane change;
- OE: the other environmental vehicles.

For a lane change segment from t_s to t_e, a *lane change data* is developed as a composition of trajectories within the period of a sequence of labeled objects (if present) and are coordinated at both the global and ego frames, where the objects are labeled on their relative position at the ego frame at time t_s.

With the ten days of experimental data across a total distance of 1232 km during on-road driving, 1596 lane changes are recorded. Because this research begins with the study on straight roads under free-flowing traffic conditions, the samples

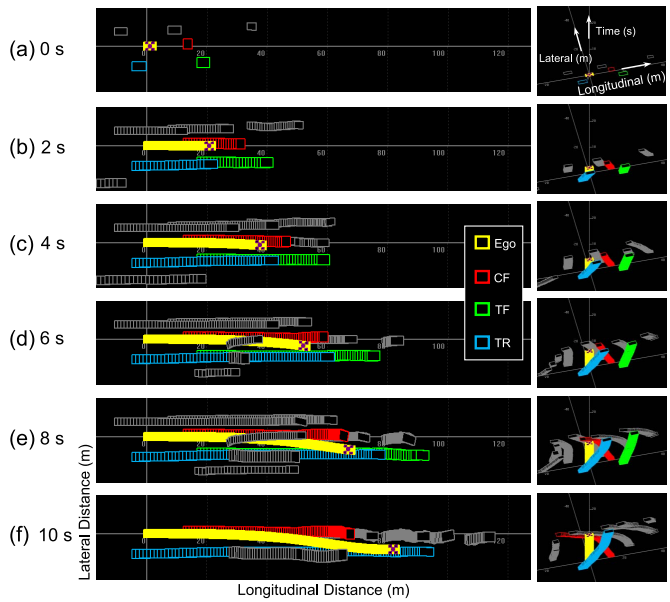

Fig. 9. Example of lane change data reproduced in time serials at (left) a global and (right) ego view.

at extremely low speeds and on curved roads are excluded. Consequently, a lane change database that contains 1006 samples is generated. As shown in Fig. 7, the set of the ego's lane change trajectories enumerate the usual paths that a driver actually follows during on-road driving. Moreover, a lane change data is shown in Fig. 9 with all trajectories that reflect the interactions of an ego and environmental vehicles during the procedure. Comparing with the data used in lane change studies in literature as listed in Table V, this database contains large amount of lane change segments that are collected during on-road driving across long distances and during long time span, and the data are constituted by the trajectories of both the ego and all interaction vehicles.

The left column of Fig. 9 presents 2D views at a global frame that illustrate the trajectories' longitudinal and lateral changes on the road. The right column are 3D views at the ego frame, showing not only paths of the ego-centered motion but also speeds. For example, in the 3D ego views, the trajectories shifting toward the road's longitudinal direction mean that the vehicles have faster speeds than the ego, and vice versa, and curved trajectories represent changes in speed. Each column plots a sequence of views across the procedure, where at a relative time δt, the trajectories within the period of $(t_s, t_s + \delta t)$ are visualized. Vehicle interactions during a right lane change procedure is clearly observed in these views. For example as depicted in the left column, TR was behind the ego at 0 s, beside the ego at 2 s and finally overtook the ego at 4 s. Additionally, the ego waited to be overtaken by the TR, then it merge into the lane behind the TR. As shown in the right column, TR was faster than both the ego and the vehicle in front of it at 2 s and 4 s, and then it slowed at 6 s when its position approached to its front.

With such lane change data, the entire procedure can be realistically reproduced, and the interactions between different vehicles can be quantitatively analyzed. A video of the data and results can be found at http://www.poss.pku.edu.cn/video.

V. Lane Change Analysis

A. Lane Change Trajectory Analysis

In many state-of-the-art autonomous driving systems, motion planning is conducted by first generating a set of trajectories then selecting one to perform that is optimal on an objective function [11]–[16]. This family of algorithms has a common basis in that a unique trajectory is generated after the two terminal states are given, although the models in use could be different. On the other hand, the set of trajectories enumerates some major candidates that could be selected for the vehicle's implementation, where the number of candidates is a key factor that affects the algorithm's accuracy and computation cost. With the vehicle's current state, proper planning of the end states is crucial. In addition to end states that address on the path of the trajectories, speed is another key factor, and they are strongly correlated.

With the set of on-road data, this research analyzes the end positions of ego vehicles' lane change trajectories by correlating with its speed. As shown in Fig. 10, the trajectories are first divided into three sets in (a) according to their speed at the start point, i.e., $V \leq 15$ m/s, 15 m/s $< V \leq 20$ m/s, and 20 m/s $< V$ for the low-, middle-and high-speeds respectively, which are found of different paths at different speed levels. For each set of trajectories, histograms and Gaussian fitting curves are generated on their end positions at both longitudinal and lateral directions in (b). It can be found that except the low-speed trajectories, which have small number of samples, the other two have Gaussian curves fitting perfectly to their histograms. For each trajectory i, a 3D end point $p_i = (s, d, v)$ is developed, where (s, d) is the end position and v is its speed at the start time. Gaussian fitting is conducted on the 3D end points in (c)∼(e), with only longitudinal and lateral axes shown, thereby providing more clear views of the distributions of the end positions. Based on the results, a 3-component GMM (Gaussian Mixture Model) is initialized, and an EM (Expectation maximization) clustering process is conducted to optimize the model and re-cluster the end points into three groups, as shown in black, blue and red in (f). In addition, a 2D view of the model on longitudinal and lateral axes is shown in (g) that depicts a probabilistic distribution of the end positions that a human driver performs in on-road driving.

Based on the above discussions, it is reasonable to assume that distribution of longitudinal and lateral displacements (s, d) at the end position of a lane change are conditioned on its initial speed v in Gaussian, with the mean and standard deviation in linear with v, i.e., $s, d|v \sim N(a_1 v + b_1, (a_2 v + b_2)^2)_{s,d}$. Given the on-road trajectories, two data sets $(v_i, s_i)_{i=1}^N$ and $(v_i, d_i)_{i=1}^N$ are generated, with which $\mathcal{A}_u = (a_1, a_2, b_1, b_2)_u$ are found respectively for $u = s, d$ on maximum likelihood estimations as below

$$\mathcal{A}_u = \arg\max_{\mathcal{A}_u} \prod_{i=1}^{N} \frac{1}{\sqrt{2\pi}(a_2 v_i + b_2)} e^{-\frac{(u_i - a_1 v_i - b_1)^2}{2(a_2 v_i + b_2)^2}} \tag{1}$$

$$= \arg\min_{\mathcal{A}_u} \sum_{i=1}^{N} \left(\ln(a_2 v_i + b_2) + \frac{2(a_2 v_i + b_2)^2}{(u_i - a_1 v_i - b_1)^2} \right). \tag{2}$$

TABLE V
COMPARISON WITH THE LANE CHANGE DATA IN LITERATURE WORKS

Research Study	Objective	Data Level	Data Collection	Description
Tehrani, 2014 [10]	drive analysis	trajectory	on-board	10.3 km on highway, 19 lane changes
Zheng, 2014 [25]	lane change detection	trajectory	infrastructure videos	877 lane changes from NGSIM datasets
Schlechtriemen, 2014 [31]	lane change detection	signal/object	on-board	1100 km and 13 hrs on highway
Satzoda, 2015 [39]	drive analysis	signal/object	on-board	35 lane changes
Satzoda, 2015 [40]	drive analysis	signal/object	on-board	65 km on highway, 2 drivers and 114 lane changes
Hou, 2014 [42]	lane change detection	trajectory	infrastructure videos	1353 lane changes from NGSIM datasets

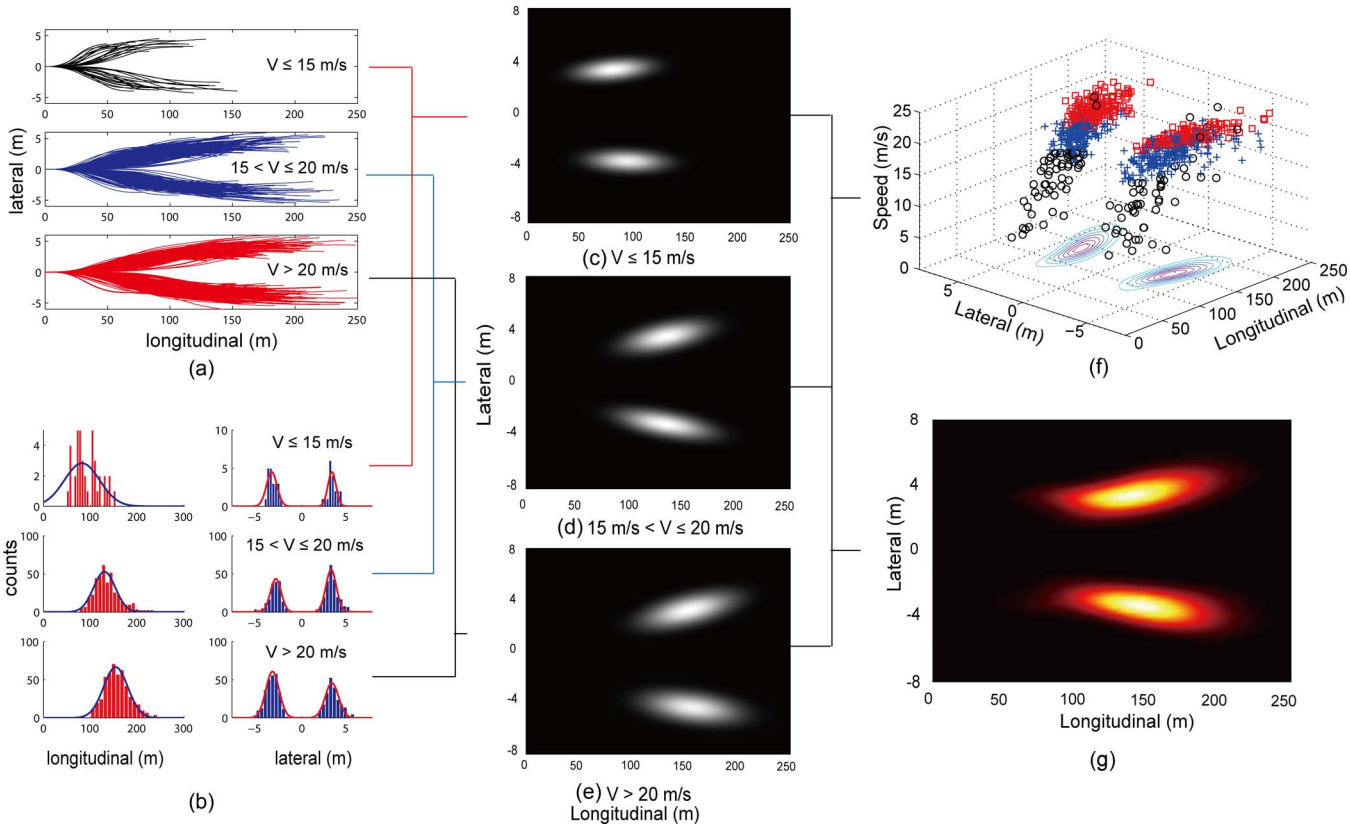

Fig. 10. Lane change trajectory analysis by correlating end points with speed.

Through a gradient-based optimization, a set of parameters are obtained with $\mathcal{A}_s = (5.99, 1.53, 40.85, 0.00)$ and $\mathcal{A}_d = (0.00, 0.00, 3.40, 0.820)$. The results are shown in Fig. 11, where left and right are the fitting results of speed with longitudinal and lateral displacements respectively, and in each sub-figure, blue line denotes the estimated mean, i.e., $a_1 v + b_1$, and two red ones are ± 2 standard deviations from the mean, i.e., $a_1 v + b_1 \pm 2(a_2 v + b_2)^2$. These results can be used to improve efficiency in end state sampling in motion planning for autonomous driving or evaluate lane changes for risk analysis or driving state awareness.

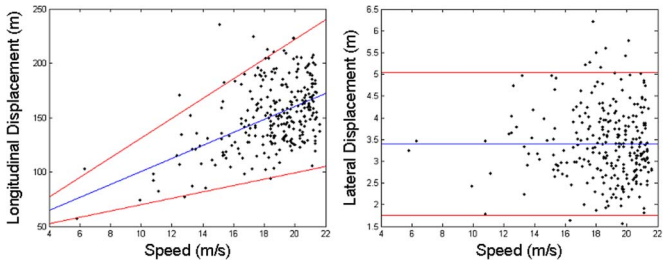

Fig. 11. Linear correlation fitting on end displacements and speed.

B. Scene-Based Lane Change Analysis

A special focus is cast on analyzing the interaction with environmental vehicles during an ego's lane change, where *interaction* is defined as below.

Definition 8: An ego is said having *interaction* with environmental vehicles during the course of its lane change, if either an environmental vehicle or the ego is forced by each other to change its former status by such as speed or lateral control, or an alternation happened in the relative position of an environmental vehicle with the ego on longitudinal direction during the procedure.

Although CF is one of the major reasons for an ego's lane change decision, uncertainties could mainly come from the environmental vehicles on the target lane. In this research, TF and TR are studied as the major interacting vehicles during an ego's lane changes. Speed or lateral control yields a result of speed or lane changes, which is reflected in the sequence of

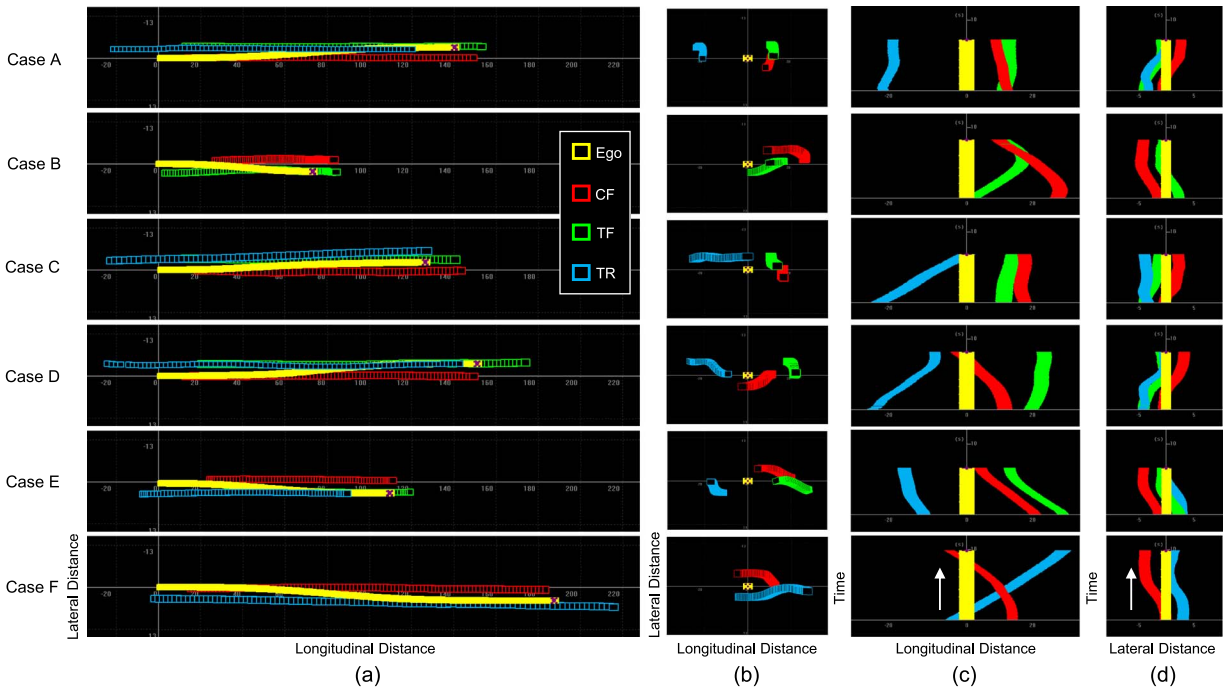

Fig. 12. Case study of different interaction types during lane changes. (a) At a global view. (b)–(d) At an ego view.

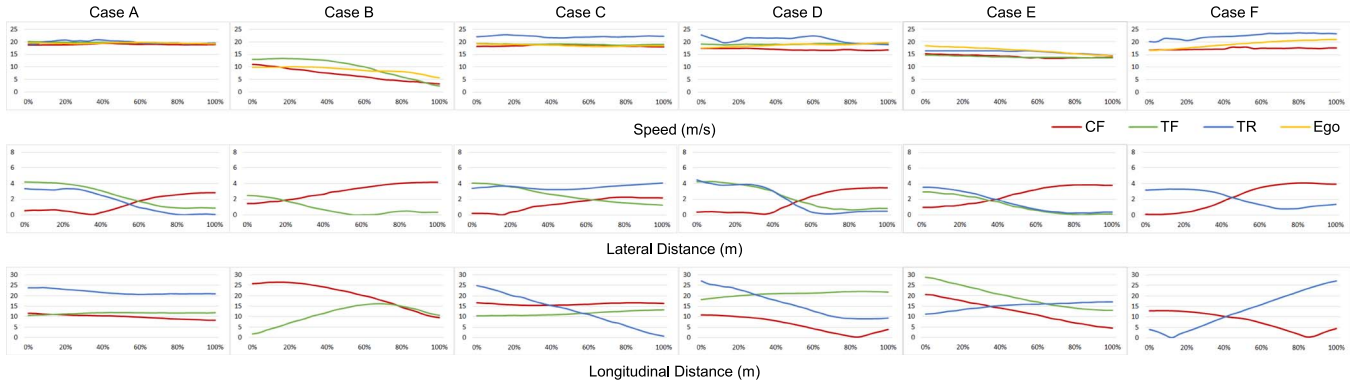

Fig. 13. Vehicle parameters of the cases in Fig. 12.

a vehicle's speed or lateral shift values. On the other hand, an environmental vehicle is labeled as TF or TR according to its positional relationship with the ego at the initial time of lane change, while it could be alternated during the procedure. For example, when an ego performs an overtaking simultaneous with lane change, a TF is changed to TR as its relative position to the ego is alternated from the ego's front to rear longitudinally. In the lane change data set, six typical cases of interactions are discovered as discussed below, with their procedures visualized in Fig. 12, and the sequences of speed, lateral and longitudinal distances with the ego plotted in Fig. 13 to represent quantitatively their time-course change as well as correlations.

Case A is the only non-interaction one. During the whole procedure, all vehicles kept their original driving status on such as speed and lane. Neither the ego nor any of an environmental vehicle was forced to make a change due to the ego's lane change, and their relative positions on longitudinal direction were maintained.

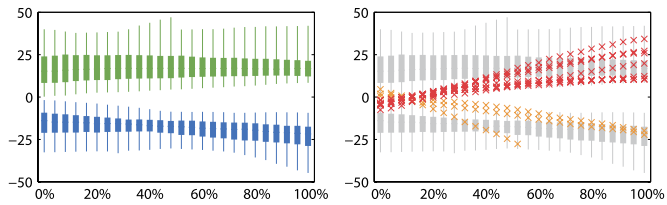

Fig. 14. Distribution of the longitudinal positions (vertical axis) of the TRs and TFs during lane change procedures (horizontal axis). (a) (Blue) TRs and (green) TFs without label change during the procedure. (b) (Red) Vehicles changed from TR to TF, or (orange) TF to TR.

Case B is an interaction one, where the ego was forced to make a speed control, following an unexpected speed down of TF due to traffic change. Although longitudinal distance of TF with the ego was close at the beginning, due to a faster speed of TF, the distance presented a tendency of being enlarged quickly, which could be a major reason for the ego's decision of a lane change. However, a slowdown of TF occurred at nearly 50% of the procedure, after which the distance was shrunk fast, and the

TABLE VI
LANE CHANGE INTERACTION MODEL

	Interaction			Example
	Type	Action	Classification Rules	
LCT1	no-interaction	none	$(TTC_0^{TF,TR} \leq 0 \ \vee \ TTC_0^{TF,TR} \geq T) \ \wedge$ $(\forall t \in [0,T], \ \Delta V_t^{EGO} < \delta\dot{s})$	case A
LCT2	unexpected-interaction	ego's behavioral change	$(TTC_0^{TF,TR} \leq 0 \ \vee \ TTC_0^{TF,TR} \geq T) \ \wedge$ $(\exists t \in [0,T], \ \Delta V_t^{EGO} \geq \delta\dot{s})$	case B
LCT3	expected-interaction	TR's behavioral change	$(0 < TTC_0^{TR} < T) \ \wedge \ (\forall t \in [0,T], \ \Delta V_t^{EGO} < \delta\dot{s}) \ \wedge$ $(\exists t \in [0,T], \ \Delta V_t^{TR} \geq \delta\dot{s} \ \vee \ \Delta D_t^{TR} \geq \delta d)$	cases C & D
LCT4	expected-interaction	ego's behavioral change	$(0 < TTC_0^{TR,TF} < T) \ \wedge$ $(\exists t \in [0,T], \ \Delta V_t^{EGO} \geq \delta\dot{s})$	case E
LCT5	expected-interaction	overtaking or overtaken	$(s_T^{TR} > s_T^{EGO}) \ \vee \ (s_T^{TF} < s_T^{EGO})$	case F

ego was forced to perform a speed down at about 80% of the procedure.

In different with Case B, Cases C–E show examples, where at the beginning of the ego's lane change, the speed of TR was much faster than the ego's with its longitudinal position approaching to the ego's, and about to collide if these vehicles keep their original driving status. Even in such situations, the ego still initiated lane changes, upon which in case C, TR maintained its former speed while performed a lane change, in case D, TR kept the lane but made a speed down, and in case E, the ego changed its speed to avoid collision.

Case F is an example, where the ego's lane change was accompanied with an overtaking or overtaken behavior, and the positional relationship of TR or TF with the ego was alternated. The procedure of such cases are further analyzed in Fig. 14. In (a), TR and TF are labeled according to their relative position at each frame with the ego, a statistics is taken on the longitudinal positions of TR and TF of all data samples at each frame during the procedure. It can be found that at the beginning of lane changes, i.e., 0%, distribute of both TRs (blue) and TFs (green) are scattered, and the two clusters are close to each other. As the procedure progressed, two clusters get more focused, and the distance between them is enlarged, which is maximized at the end, i.e., 100%. Such a distance represents the space in between of the environmental vehicles on the target lane to let the ego merged in. With (a) as a background, the samples of cases E and F are emphasized in (b). It can be found that positional alternation are finished at an early part of the procedure, and the longitudinal positions of TR and TF present linear changes, meaning that their initial driving status are maintained during the procedure.

Based on the above discussions, interactions between an ego with scene vehicles during its lane change are modeled into five types as detailed in Table VI. LCT1 corresponds to case A, where the ego keeps its speed during the course, and if the environmental vehicles maintain their original driving status, there is no risk of collision. In such a situation, even an environmental vehicle made speed or lane change, it is considered not directly caused by the ego's lane change. LCT2 corresponds to case B, where an ego is forced to make speed control, which is unexpected and should not be necessary if the environmental vehicles maintain their original driving status. So that LCT2 is typed of an unexpected-interaction. In different with LCT2, the interactions of LCT3–5 could be expected by the ego at the beginning of lane changes, so that typed of expected-interaction. LCT3 corresponds to cases C and D, where TR is forced to change its former driving status, while LCT4 is on the contrary, corresponding to case E with a speed change occurred in the ego. LCT5 corresponds to case F, where an overtaking or overtaken is accompanied with the ego's lane change. In different with LCT3–4, the original driving status are maintained by both the ego and environmental vehicles in LCT5.

Classification rules are defined in Table VI on the above addressed interaction types. In this research, TTC (Time To Contact) is used to examine whether an interaction with a certain environmental vehicle (TR or TF) could be expected by an ego. Denoting a trajectory point at time t by $p_t = (s_t, d_t)$ at a global frame, and $t = 0$ for the initial time of a lane change, TTC is defined below

$$\mathrm{TTC}_0^{\mathrm{TF,TR}} = \frac{\left(s_0^{\mathrm{TF,TR}} - s_0^{\mathrm{EGO}}\right)}{\left(\dot{s}_0^{\mathrm{TF,TR}} - \dot{s}_0^{\mathrm{EGO}}\right)}. \tag{3}$$

An interaction is predicted, if $0 < \mathrm{TTC}_0^{\mathrm{TF}} < T$ or $0 < \mathrm{TTC}_0^{\mathrm{TR}} < T$, where $T = 8$ s is the average lane change duration. On the other hand, given an initial state $P_0 = [p_0, \dot{p}_0, \ddot{p}_0]$ consisting of a TR or TF's location, speed and acceleration, a predicted state $P_t = [p'_t, \dot{p}'_t, \ddot{p}'_t = \ddot{p}_0]$ at time t is estimated by assuming on a linear motion, with $p'_t = (s'_k, d'_k)$ and $\dot{p}'_t = (\dot{s}'_t, \dot{d}'_t)$, and changes on speed (ΔV_t) and lateral position (ΔD_t) are estimated below. A speed or lateral position change is detected during a lane change procedure, if there exists a $t \in [0, T]$s that has $\Delta V_t \geq \delta\dot{s}$ or $\Delta D_t \geq \delta d$, where $\delta\dot{s}$ and δd are predefined thresholds. Only speed change is detected for the ego in the same way

$$\Delta V_t = \max\left(\left\|\dot{s}'_t - \dot{s}_t\right\|, \left\|\dot{d}'_t - \dot{d}_t\right\|\right) \tag{4}$$

$$\Delta D_t = \left\|d'_t - d_t\right\|. \tag{5}$$

Based on these classification rules, the lane change samples are classified into LCT1–5 as listed in Table VII, with the ego's trajectories visualized in Fig. 15. It is obvious that LCT1 is of the majority, while no generalization can be developed confidently on the differences of the five sets based only on their visualization. On the other hand, many methods have been developed in literature of trajectory generation for motion

TABLE VII
RESULT OF INTERACTION-BASED LANE CHANGE CLASSIFICATION

	Samples	Percentage	Err Mean (m)	Err Mean (Norm.)
LCT1	724	72.0%	1.535	1.10%
LCT2	119	11.8%	3.350	2.53%
LCT3	31	3.1%	1.898	1.43%
LCT4	17	1.7%	2.480	2.17%
LCT5	112	11.1%	2.982	2.07%

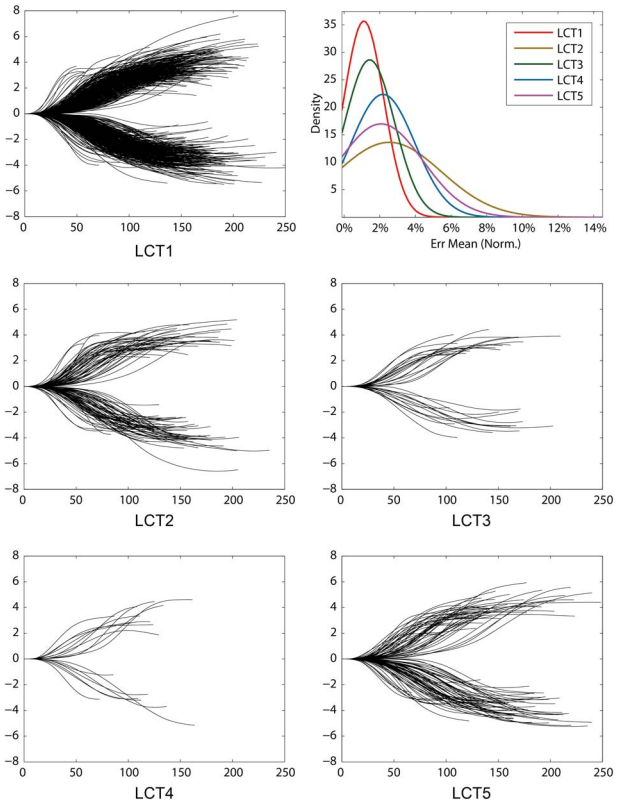

Fig. 15. Classification of the lane change trajectories on their interaction types and error evaluation.

planning or risk analysis [11]–[16], while these methods do not take into account scene vehicles in estimating a trajectory connecting a start and end state. Such synthesized trajectories can be used to establish a baseline in evaluating real world ones. In this research, the trajectory generation method [8], [43] is used, which plan two quintic polynomials on lateral and longitudinal axes respectively. Given two states (P_0, P_T) of an ego's lane change trajectory at its initial $t = 0$ and end times $t = T$, where $P_t = [p_t = (s_t, d_t), \dot{p}_t = (\dot{s}_t, \dot{d}_t), \ddot{p}_t = (\ddot{s}_t, \ddot{d}_t)]$, a synthesized trajectory is developed as defined below by fitting the coefficients $a_0, \ldots, a_5$ and $b_0, \ldots, b_5$ constrained on the two given states

$$d_t = a_0 + a_1 t + a_2 t^2 + a_3 t^3 + a_4 t^4 + a_5 t^5 \quad (6)$$

$$s_t = b_0 + b_1 t + b_2 t^2 + b_3 t^3 + b_4 t^4 + b_5 t^5. \quad (7)$$

A residual is estimated as the Euclidean distance at each time instance of a real trajectory to its synchronized position of the synthesized one, and an error measure is defined for each real trajectory as the standard deviation of the residuals during its entire span. Such an error measure is further normalized by dividing the longitudinal length of the trajectory. For each set of trajectories, a mean error and a normalized mean error are estimated as listed in Table VII, and Gaussian curves are fitted on the normalized errors as shown in Fig. 15. It can be found that LCT1 has the lowest error, meaning that a trajectory generated using a state-of-the-art method has high accuracy in synthesizing the one at real situations when no interaction with scene vehicles occurs, which possesses 72.0% of the total data set. For the rest 28.0% of trajectories of LCT2–5, where the ego have interactions with scene vehicles during lane changes, errors are much larger. However among them, the interactions of LCT3-5 can be expected by the ego at its initial time of lane changes, which possess 16.2% of the total data set, and therefore can be synthesized with improved accuracy by developing new trajectory generation methods that incorporating different types of interactions with scene objects. Such methods will be addressed in our future work. LCT2 is the only type, where interactions could not be predicted when the ego initiated lane changes, which possesses 11.8% of the total data set and shows the largest error between real-world trajectories and synthesized ones. It prompts that risk analysis is always needed, even if safety has been confirmed at the beginning of lane changes.

VI. CONCLUSION

Based on the results of Part I on on-road vehicle trajectory collection, this article has addressed lane change extraction and scene-based behavior analysis, which is the second part of a two-part work for a tactical-level on-road lane change behavior study. In this work, an automatic method is proposed for extracting lane change segments from a continuous driving sequence by modeling and recognizing patterns in steering angle, and through large-scale on-road data collection and processing, a lane change database is generated that reflects the interactions at the trajectory level between an ego and surrounding vehicles across the entire procedure. Lane change procedures are analyzed, where a trajectory model is developed by cross-correlating the spatial-temporal features on the trajectory's end location and speed, and an interaction model is derived to classify lane changes and predict their interactions by cross-correlating the ego with other scene vehicles. To the authors' knowledge, this is the first work to study lane change behaviors from an on-road perspective that addresses the vehicle interactions in real-world traffic at the trajectory level, and the findings will help in developing future ADAS or autonomous driving systems to govern safe and gentle social behaviors in dynamic traffic.

REFERENCES

[1] J. A. Michon, "A critical view of driver behavior models: What do we know, what should we do?" in *Human Behavior and Traffic Safety*, L. Evans and R. C. Schwing, Eds. New York, NY, USA: Plenum, 1985, pp. 485–520.
[2] J. Wei, J. M. Dolan, and B. Litkouhi, "A point-based MDP for robust single-lane autonomous driving behavior under uncertainties," in *Proc. IEEE Int. Conf. Robot. Autom.*, 2011, pp. 2586–2592.
[3] J. Lu, D. Filev, and F. Tseng "Real-time determination of driver's driving behavior during car following," *SAE Int. J. Passenger Cars-Electron. Elect. Syst.*, vol. 8, no. 2, pp. 371–378, 2015.
[4] A. Broggi, P. Cerri, M. Felisa, M. C. Laghi, L. Mazzei, and P. P. Porta, "The vislab intercontinental autonomous challenge: An extensive test for a platoon of intelligent vehicles," *Int. J. Veh. Auton. Syst.*, vol. 10, no. 3, pp. 147–164, 2012.

[5] M. Gouy, K. Wiedemann, A. Stevens, G. Brunett, and N. Reed, "Driving next to automated vehicle platoons: How do short time headways influence non-platoon drivers longitudinal control?" *Transp. Res. F, Traffic Psychol. Behav.*, vol. 27, pp. 264–273, Nov. 2014.
[6] A. Ghaffari, A. Khodayari, S. Arvin, and F. Alimardani, "Lane change trajectory model considering the driver effects based on MANFIS," *Int. J. Automot. Eng.*, vol. 2, no. 4, pp. 261–275, 2012.
[7] J. Levinson *et al.*, "Towards fully autonomous driving: Systems and algorithms," in *Proc. IEEE Intell. Veh. Symp.*, 2011, pp. 163–168.
[8] M. Werling, S. Kammel, J. Ziegler, and L. Groll, "Optimal trajectories for time-critical street scenarios using discretized terminal manifolds," *Int. J. Robot. Res.*, vol. 31, no. 3, pp. 346–359, 2012.
[9] J. Ziegler, P. Bender, T. Dang, and C. Stiller, "Trajectory planning for Bertha—A local, continuous method," in *Proc. IEEE Intell. Veh. Symp.*, 2014, pp. 450–457.
[10] H. Tehrani, K. Muto, K. Yoneda, and S. Mita, "Evaluating human & computer for expressway lane changing," in *Proc. IEEE Intell. Veh. Symp.*, 2014, pp. 382–387.
[11] A. Geiger *et al.*, "Team Annieway's entry to the 2011 grand cooperative driving challenge," *IEEE J. Intell. Transp. Syst.*, vol. 13, no. 3, pp. 1008–1017, Sep. 2012.
[12] T. M. Howard, M. Pivtoraiko, R. Knepper, and A. Kelly, "Model-predictive motion planning: Several key developments for autonomous mobile robots," *IEEE Robot. Autom. Mag.*, vol. 21, no. 1, pp. 64–73, Mar. 2014.
[13] J. Huber, C. Gruber, and M. Hofbaur, "Online trajectory optimization for nonlinear systems by the concept of a model control loop—Applied to the reaction wheel pendulum," in *Proc. IEEE Int. Conf. Control Appl.*, 2013, pp. 935–940.
[14] A. Lawitzky, D. Althoff, C. F. Passenberg, G. Tanzmeister, D. Wollherr, and M. Buss, "Interactive scene prediction for automotive applications," in *Proc. IEEE Intell. Veh. Symp.*, 2013, pp. 1028–1033.
[15] C. Rathgeber, F. Winkler, D. Odenthal, and S. Muller, "Lateral trajectory tracking control for autonomous vehicles," in *Proc. IEEE Eur. Control Conf.*, 2014, pp. 1024–1029.
[16] W. Xu, J. Pan, J. Wei, and J. M. Dolan, "Motion planning under uncertainty for on-road autonomous driving," in *Proc. IEEE Int. Conf. Robot. Autom.*, 2014, pp. 2507–2512.
[17] J. Lee, N. Ward, E. Boer, T. Brown, S. Balk, and O. Ahmad "Making driving simulators more useful for behavioral research—Simulator characteristics comparison and model-based transformation," Univ. IOWA, Iowa City, IA, USA, Project Rep. N2013-016, 2013.
[18] N. P. Belz and L. Aultman-Hall, "Implementation, Driver Behavior, and Simulation: Issues Related to Roundabouts in Northern New England," Nat. Tech. Inf. Service, Alexandria, VA, USA, UVM TRC Rep. 14-003, 2014.
[19] L. Wan, P. Raksincharoensak, K. Maeda, and M. Nagai, "Lane change behavior modeling for autonomous vehicles based on surroundings recognition," *Int. J. Automot. Eng.*, vol. 2, no. 2, pp. 7–12, 2011.
[20] V. Kovvali, V. Alexiadis, and L. Zhang, "Video-based vehicle trajectory data collection," in *Proc. Annu. Meet. Transp. Res. Rec.*, 2007, pp. 1–18.
[21] *The Next Generation Simulation Program (NGSIM)*. [Online]. Available: http://ngsim-community.org/
[22] S. Moridpour, G. Rose, and M. Sarvi, "Effect of surrounding traffic characteristics on lane changing behavior," *J. Transp. Eng.*, vol. 136, no. 11, pp. 973–985, 2010.
[23] H. N. Koutsopoulos, and H. Farah, "Latent class model for car-following behavior," *Transp. Res. B*, vol. 46, no. 5, pp. 563–578, 2012.
[24] M. Montanino and V. Punzo, "Making NGSIM data usable for studies on traffic flow theory: Multistep method for vehicle trajectory reconstruction," *J. Transp. Res. Board*, vol. 2390, pp. 99–111, 2013.
[25] J. Zheng, K. Suzuki, and M. Fujita, "Predicting drivers lane-changing decisions using a neural network model," in *Proc. IEEE Intell. Veh. Symp.*, 2014, pp. 108–114.
[26] S. Moridpour, E. Mazloumi, and M. Mesbah, "Impact of heavy vehicles on surrounding traffic characteristics," *J. Adv. Transp.*, vol. 49, no. 4, pp. 535–552, 2014.
[27] S. Lefevre, D. Vasquez, and C. Laugier, "A survey on motion prediction and risk assessment for intelligent vehicles," *ROBOMECH J.*, vol. 1, no. 1, pp. 1–14, 2014.
[28] N. Oliver and A. P. Pentland, "Driver behavior recognition and prediction in a SmartCar," in *Proc. SPIE Aerosense-Enhanced Synthetic Vis.*, 2000, pp. 280–290.
[29] B. Morris, A. Doshi, and M. M. Trivedi, "Lane change intent prediction for driver assistance: On-road design and evaluation," in *Proc. IEEE Intell. Veh. Symp.*, 2011, pp. 895–901.
[30] P. Kumar, M. Perrollaz, S. Lefevre, and C. Laugier, "Learning-based approach for online lane change intention prediction," in *Proc. IEEE Intell. Veh. Symp.*, 2013, pp. 797–802.
[31] J. Schlechtriemen, A. Wedel, J. Hillenbrand, G. Breuel, and K.-D. Kuhnert, "A lane change detection approach using feature ranking with maximized predictive power," *Simul. Model. Practice Theory*, vol. 42, pp. 73–83, 2014.
[32] M. Mori, C. Miyajima, T. Hirayama, and N. Kitaoka, "Integrated modeling of driver gaze and vehicle operation behavior to estimate risk level during lane changes," in *Proc. IEEE Int. Conf. Intell. Transp. Syst.*, 2013, pp. 2020–2025.
[33] C. Hill, L. Elefteriadou, and A. Kondyli, "Exploratory analysis of lane changing on freeways based on driver behavior," *J. Transp. Eng.*, vol. 141, no. 4, 2015, Art. no. 04014090.
[34] V. L. Neale, T. A. Dingus, S. G. Klauer, J. Sudweeks, and M. Goodman, "An overview of the 100-car naturalistic driving study and findings," in *Proc. 19th Int. Tech. Conf. Enhanc. Safety Veh.*, 2005, pp. 1–10.
[35] K. L. Campbell, "The SHRP 2 naturalistic driving study: Addressing driver performance and behavior in traffic safety," *TR News*, vol. 282, pp. 30–35, 2012.
[36] M. A. Regan *et al.*, "The Australian 400-car naturalistic driving study: Innovation in road safety research and policy," in *Proc. Australasian Road Safety Res., Policing Educ. Conf.*, 2013, pp. 1–13.
[37] R. Eeninka, Y. Barnardb, M. Baumannc, X. Augrosd, and F. Uteschc, "UDRIVE: The European naturalistic driving study," in *Proc. Transp. Res. Arena*, 2014, pp. 1–10.
[38] R. K. Satzoda and M. M. Trivedi, "Overtaking & Receding vehicle detection for driver assistance and naturalistic driving studies," in *Proc. IEEE Int. Conf. ITSC*, 2014, pp. 697–702.
[39] R. K. Satzoda, P. Gunaratne, and M. M. Trivedi, "Drive quality analysis of lane change maneuvers for naturalistic driving studies," in *Proc. IEEE Intell. Veh. Symp.*, 2015, pp. 654–659.
[40] R. K. Satzoda and M. M. Trivedi, "Drive analysis using vehicle dynamics and vision-based lane semantics," *IEEE Trans. Intell. Transp. Syst.*, vol. 16, no. 1, pp. 9–18, Feb. 2015.
[41] W. Yao, H. Zhao, F. Davoine, and H. Zha, "Learning lane change trajectories from on-road driving data," in *Proc. IEEE Intell. Veh. Symp.*, 2012, pp. 885–890.
[42] Y. Hou, P. Edara, and C. Sun, "Modeling mandatory lane changing using Bayes classifier and decision trees," *IEEE Trans. Intell. Transp. Syst.*, vol. 15, no. 2, pp. 647–655, Apr. 2014.
[43] W. Xu, W. Yao, H. Zhao, and H. Zha, "A vehicle model for micro-traffic simulation in dynamic urban scenarios," in *Proc. IEEE Int. Conf. Robot. Autom.*, 2011, pp. 2267–2274.

Wen Yao received the B.S. degree in automation from Tsinghua University, Beijing, China, in 2009 and the Ph.D. degree in intelligent science and technology in 2015 from Peking University, Beijing.

He is now working with China North Vehicle Research Institute, Beijing. He is also with the Key Laboratory of Machine Perception (Ministry of Education), Peking University, Beijing. His research interests include intelligent vehicle, behavior learning, and motion planning for mobile robots.

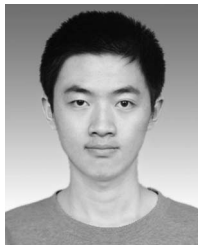

Qiqi Zeng received the B.S. degree in intelligent science and technology from Peking University, Beijing, China, in 2013, where he is currently working toward the Ph.D. degree in computer science in the Key Laboratory of Machine Perception (Ministry of Education).

His research interests include computer vision, intelligent vehicle, and traffic activities understanding.

Yuping Lin received the B.S. degree in electrical engineering from Sun Yat-Sen University, Kaohsiung, Taiwan, in 1997, the M.S. degree in mechanical engineering from Tatung University, Taipei, Taiwan, in 2004, and the M.S. degree in computer science from the University of Detroit Mercy, Detroit, MI, USA, in 2007. He is currently working toward the Ph.D. degree in the Key Laboratory of Machine Perception (Ministry of Education), Peking University, Beijing, China.

His research interests include computer vision and machine perception.

Donghao Xu received the B.S. degree in information and computing science from Peking University, Beijing, China, in 2012, where he is currently working toward the Ph.D. degree in computer science in the Key Laboratory of Machine Perception (Ministry of Education).

His research interests include computer vision, machine learning, and intelligent vehicles.

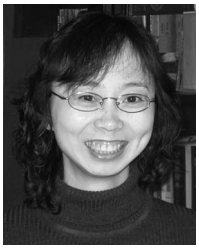

Huijing Zhao received the B.S. degree in computer science from Peking University, Beijing, China, in 1991 and the M.E. and Ph.D. degrees in civil engineering from the University of Tokyo, Tokyo, Japan, in 1996 and 1999, respectively.

From 1991 to 1994, she was recruited by Peking University in a project of developing a geographic information system platform. In 2003, after several years of postdoctoral research with the University of Tokyo, she became a Visiting Associate Professor with the Center for Spatial Information Science. In 2007, she joined Peking University as an Associate Professor with the School of Electronics Engineering and Computer Science. Her research interests include intelligent vehicle, machine perception, and mobile robots.

Franck Guillemard was born in France on March 18, 1968. He received the Ph.D. degree in control engineering from the University of Lille, Lille, France, in 1996.

Currently, he is with the Scientific Department of Groupe PSA (Peugeot Société Anonyme), where he is in charge of advanced research concerning computing science, electronics, and photonics and control. He is also an expert in the field of modeling, design, and control of automotive mechatronic systems.

Stéphane Geronimi received the Ph.D. degree in physics and optronics from the University of Paris XI, Orsay, France, in 1996.

He joined the Groupe PSA (Peugeot Société Anonyme) in 2000. Since then, he has been involved in several research projects in the domain of driver assistance systems. He has been in charge of innovation projects dealing with advanced driver assistance systems (ADAS). He is currently an expert in ADAS and safety for ADAS and is working on the automation of driving functions.

François Aioun received the engineering degree in electronics, computer science, and automatic control from the École Supérieure d'Informatique, Électronique, Automatique High School, Paris, France, in 1988, the Postgraduate Diploma in automatic control and signal processing in 1989, and the Ph.D. degree in automatic control in 1993.

From 1989 to 1993, he was recruited by Electricité de France to study active vibration control of a structure. After the postdoctoral research at Ecole Normale Supérieure of Cachan, Cachan, France, and in different companies, he joined the Groupe PSA (Peugeot Société Anonyme) in 1997. His research interests in automatic control cover active vibration, power plant, powertrain, actuators, and more recently, autonomous and intelligent vehicles.